

# A thermodynamically consistent poro-visco-elastic model of Extracellular Matrix

Giulia Laura Celora

Mathematical Institute, University of Oxford

**Abstract.**

## 1 Introduction

There are several studies supporting the central role of mechanical stimuli in tissue morphogenesis and homeostasis [5,40]. In tissues, cells are mainly surrounded by extracellular matrix (ECM), a soft porous media made up of networks of polymer chains and proteins. *In vitro* studies have shown that ECM rigidity and shear stresses can alone promote malignant phenotypes in a population of initially normal cells, impact on cell proliferation and differentiation [9]. Further experiments on solid tumour development have proven that this is often associated to a stiffening of the tissue compared to the surrounding healthy one [38], which results in the exposure of cells to higher compressive stresses as well as favouring the collapse of blood vessels and impeding the diffusion of substances in the extra-cellular environment ultimately decreasing the efficacy of numerous therapies [44]. Based on such evidence, it is now widely accepted that, unlike originally thought, biological processes are not simply regulated by biochemical signals but by the complex interplay of mechanical and chemical stimuli.

Given the different physical nature and scale of phenomena involved, coupling micro-environment and cell behaviours is a problem of high complexity. This requires understanding processes occurring at different temporal and spatial scales and how they interplay to determine the macroscopic behaviour of a tissue, whether healthy or damaged. If we can learn to tune its properties, as cells already do, this could lead to the development of novel therapies and completely change our approach to drug design. In order for this to be possible, alongside experiments, it is necessary to develop a theoretical framework able to capture both the biology and physics involved and which is consistent with the known universal laws of Nature [28].

With the development of new experimental techniques such as Atomic Force Microscopy (AFM), the local mechanical properties of a material can be measured with atomic precision [26]. When tested at this scale, soft tissues and the ECM in particular have been found to be visco-elastic [32]. Purely elastic solids only store energy when deformed, viscoelastic material instead exhibit a time-dependent response as part of the energy is dissipated in the deformation process. While a large amount of literature focuses on the elastic properties of

ECM, it remains unclear the role of viscosity in determining cell behaviour. However, the recent efforts to develop synthetic ECM, i.e. hydrogels, with tunable viscoelasticity, have now opened new research opportunities [12].

Despite the progress in experimental techniques, theoretical studies of viscoelastic soft materials remain limited. While experiments rapidly progress, most of the literature on mathematical modelling for soft matter has completely neglected viscous dissipation [10]. Whether this assumption might be valid for certain applications, the empirical studies previously mentioned highlight the need of including this component in the study of living tissues. Our work aims to develop a continuum mathematical model of the extracellular matrix which is consistent with the laws of thermodynamics, which accounts for its poro-visco-elastic properties and the coupling of mechanical, transport and electrical phenomena. At our present knowledge, there is no previous work in the literature capturing all these aspects. In [43,44] Xue et al. develop a nonlinear poroelastic theory for ECM, which couples all three physical phenomena but does not include viscous dissipation. In [20], the authors couple mechano-electrophysiological effects including the viscous dissipation but neglect transport; Caccavo et al. [10] propose a poro-viscoelastic model for neutral hydrogel, thus excluding electrical effects. Following these previous work, we will derive our model in the framework of linear non-equilibrium thermodynamics [28], multi-phase modelling and Biot's poroelastic theory of continuum [6].

Despite the large number of studies that have characterised the poro-elastic and visco-elastic properties of ECM independently, little is known about their combined effect. In the literature, two main constitutive models have been presented, but never rigorously compared. Instead of arbitrarily choosing one of the two, we here rely on both approaches, with the aim of identifying their differences and investigating experimental result which would allow us to experimentally test which one best describes the behaviour of soft tissues. From this point of view, our results are more widely applicable to the study of polyelectrolyte gels, which are largely applied as biomedical devices and as a synthetic equivalent of ECM.

Our work is organized as follows: in Section 2 we start with a brief overview of Classical Irreversible Thermodynamics. After presenting the composition of the ECM, Section 4 will be focusing on the derivation of the governing equation for the deformation and swelling of ECM. [... FOLLOWING SECTIONS TO UPDATE AS I WRITE.]

## 2 Non Equilibrium Thermodynamics.

While equilibrium thermodynamics can describe ideal processes, it does not apply to real processes which are irreversible. In this cases, the change in the entropy of a system  $dS$  results from both the reversible exchange of energy and matter with the external environment  $d_e S$  and the internal dissipation of energy during the process  $d_i S$  [28]:

$$dS = d_e S + d_i S, \quad (1)$$

According to the second law of thermodynamics, which applies universally to any system or any of its sub-part  $dS_i \geq 0$ . It is important to notice that the second law allows transformations in which total change in entropy  $dS$  of the system is negative. This occurs whenever  $-d_e S > d_i S$  and it can lead to the spontaneous formation of complex and ordered structures such as living organisms. From this point of view, life has emerged as an efficient mechanism able to increase sufficiently the entropy of its environment [35].

In this study, we will focus on isothermal processes, i.e.  $T = \text{const.}$  Under this assumption, as derived by Gurtin in [22], the second law of thermodynamics is equivalent to the following *energy imbalance inequality*:

$$\frac{d}{dt} \left\{ \int_R \psi \right\} \leq W(R) + M(R) \quad (2)$$

where  $R$  is a arbitrary control volume of the system,  $\psi$  is the Helmholtz free energy,  $W(R)$  is the rate at which the environment does work on  $R$  and  $M(R)$  is the inflow of mass due to transport. It is important to note that, as long as the quantities involved are well defined, the energy inequality (2) holds for any isothermal process independently of the specific physical system considered. This imposes a constraint on the form of the function  $\psi$  and how this depends on the other thermodynamic variables, such as temperature or pressure, which are used to describe the system.

Non-equilibrium thermodynamics mainly focuses on defining the form of  $d_i S$ , which, unlike the reversible entropy production  $d_e S$ , is not a state variable but depends on the specific transformation applied to the system. Different theories have been proposed, [28], each with its assumptions and specific domain of applicability. In our study we will focus on “Classical Irreversible Thermodynamics” (CIT) which was pioneered by Onsager [37] and Prigogine [39] in the first half of the 20th century. One the most important assumptions of this theory is the *Local Equilibrium Hypothesis*, which guarantees thermodynamic variables, including entropy, are locally well-defined, [28]. Consequently, we can introduce the entropy density  $s = s(\mathbf{x}, t)$  such that:

$$S = \int_R s \, dV, \quad ds = d_e s + d_i s, \quad d_i s > 0, \quad (3)$$

and the local entropy production:

$$\sigma \equiv \frac{d_i s}{dt} \geq 0. \quad (4)$$

Another central aspect of the theory is the introduction of *thermodynamic forces* <sup>1</sup>  $F_m$  (causes) and *thermodynamic fluxes*  $J_m$  (effects) to describe the time evolution of the system during an irreversible transformation. These are related to  $\sigma$  as follows:

$$\sigma = \sum_m F_m J_m. \quad (5)$$

---

<sup>1</sup> Not to be intended in the mechanical sense

While the local equilibrium hypothesis is at the basis of most theories of non-equilibrium thermodynamics, the following two hypotheses uniquely identify CIT:

1. *Linear Relation between forces  $F$  and fluxes  $J$ :*

$$J_m = \sum_k L_{mk} F_k, \quad (6)$$

where the constant  $L_{mk}$  are referred to as **phenomenological coefficients**;

2. *Microscopic Reversibility:* time reversibility of processes at the micro-scale.

Starting from these two principles, in its seminal paper [37] Onsager derives the well-known *Onsager Reciprocal Relation*:

$$L_{mk} = L_{km}. \quad (7)$$

If we now consider an isothermal transformation in the framework of CIT, alongside with the energy imbalance inequality, we have that the following must hold:

$$W(R) + M(R) - \frac{d}{dt} \left\{ \int_R \psi \right\} = T \int_R \sigma dV \quad (8)$$

In the past few decades, CIT has been applied successfully to the modelling of several physical phenomena of interest for engineers, physicists and applied mathematicians. However, its validity is limited to phenomena near-equilibrium, for which a linear approximation of the flux-force relation holds. The growing interest in more complex far-from-equilibrium phenomena has pushed toward the development of a more general framework for the study of a non-equilibrium phenomena. Since this goes beyond the purpose of our study, we will not discuss it further. We just want to mention the law of steepest entropy ascent, which, according to Beretta [3], seems to emerge as the fourth fundamental law of nature. In the linear regime, this principle can be used to prove Onsager's reciprocal relation [2], with no reference to the microscopic reversibility hypothesis, whose validity remains instead controversial [31].

### 3 Composition of Extracellular Matrix.

Despite the tissue-specific nature of Extracellular Matrix (ECM), as shown in Figure 1 (a), this is usually composed of a network of collagen fibrils entangled with proteoglycans (PGAs) which are covalently bonded to charged chains of glycosaminoglycans (GAGs). While collagen is mainly responsible for the mechanical behaviour of the tissue, GAGs can imbibe water, giving the extracellular matrix the ability to swell while maintaining its structural integrity. From this point of view, the ECM behaves as a polyelectrolyte gel [43,44]. As schematically illustrated in Figure 1(b), polyelectrolyte gels are 3D networks of cross-linked polymer chains that contain ionizable functional groups. When in solution the

gel swells, while the functional groups dissociate into fixed charges and mobile ions in the solution. Besides being largely present in the natural world, synthetic polyelectrolytes are currently employed for a wide range of applications, such as drug delivery, biomedical devices, scaffolds for tissue engineering and soft robotics [8,13,14,33]. Given their wide industrial application, there has been a growing effort in understanding their behaviour and translating it into mathematical models. In particular, research has been focusing on the phenomena of swelling, i.e. large deformation due to absorption of water, and the diffusion transport and release of solution [16,17,24,45]. However, only a small fraction of the study published accounts for the visco-elastic properties of the polymer network. As shown in Figure 1, the extracellular matrix falls into the definition

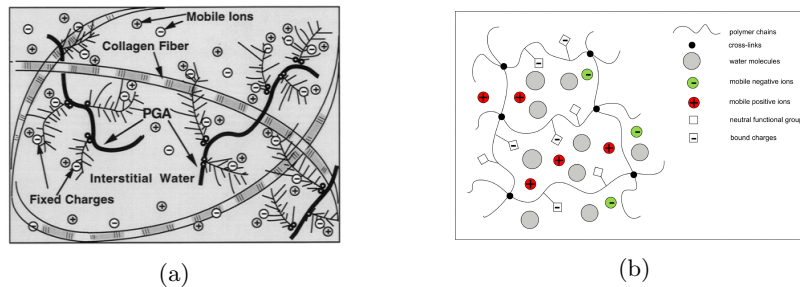


Fig. 1: Analogy between ECM in soft tissue and polyelectrolytes hydrogels: (a) schematic diagram of the structure of the charged hydrated articular cartilage, reproduced from [41]; (b) an anionic polyelectrolyte gel modelled as a three-phase continuum, reproduced from [17].

of polyelectrolytes so that the knowledge acquired in the study of these materials can be transferred to soft tissues. For the purpose of this study, we will not explicitly distinguish between collagen, PGAs and GAGs. At the tissue level, this can be grouped into a single solid phase (the polymer networks), whose mechanical properties are treated as the average over the different components contribution. As common in multiphase models of tissue, we will assume that the matrix is isotropic and GAGs are evenly distributed on the network. While this is not a good approximation for tissue like cartilage, which are highly anisotropic, it does apply to the extracellular matrix found in other soft tissue like liver, brain and tumours. It is also important to point out that ECM has additional properties such as thermo-sensitivity and pH-sensitivity. However, both in living organisms and in experimental set-up temperature and pH are maintained fairly constant.

## 4 Model Development

### 4.1 Conservation Law.

As mentioned in the previous section, we here consider the ECM as a three-phase medium composed of a solid polymer network with fixed charges, a solvent (i.e. water molecules, interstitial fluid) and solutes (freely moving charges).

We assume that the deformation of the ECM corresponds to the one of the solid network. As the tissue deform, the material element originally located at  $\mathbf{X}$  in the initial configuration  $\mathcal{B}_0$  is displaced to the point  $\mathbf{x}$  in the current configuration  $\mathcal{B}$ . Such transformation is described by the deformation gradient tensor  $\mathbb{F} = \partial \mathbf{x} / \partial \mathbf{X}$ ; the information about the change in ECM's volume due is encoded by  $J = \det \mathbb{F}$ . Since we assume the solid phase to be incompressible, any change in the volume can only be related to the migration of solvent and solutes molecules, whose nominal concentrations will be denoted by  $C_s$  and  $C_i$  respectively,  $i = 1, \dots, N$  with  $N$  being the number of free ion species. This lead to the molecular incompressibility condition:

$$J = 1 + v_s C_s + \sum_{i=1}^N v_i C_i \quad (9)$$

where  $v_m$  are the characteristic molecular volume of each species in the solution. When considering the interstitial fluid, the contribution of ions to the volume can be neglected [43,44] so that Equation (9) reduces to:

$$J = 1 + v_s C_s. \quad (10)$$

Consequently, the volume fractions of fluid  $\phi_f$  and solid  $\phi_n$  phases in the gel are defined as:

$$\phi_f = \frac{v_s C_s}{1 + v_s C_s}, \quad \phi_n = \frac{1}{1 + v_s C_s}. \quad (11)$$

where again we are neglecting the contribution of ions to the total volume. While  $C_m$  denote the number of each molecule per unit volume in the initial configuration for the  $m$ -th species in the solution, the actual concentration in the current state is denoted by  $c_m = C_m / J$ . Throughout the derivation of the model, we will be using the index  $i = 1, \dots, N$  to denote the ionic species only, while  $m \in \{s, 1, \dots, N\}$  to refer to all mobile species, i.e. both the solvent and solutes.

Mass conservation must apply to all mobile species and in the initial configuration this reads:

$$\dot{C}_m + \nabla_0 \cdot \mathbf{J}_m = 0, \quad (12)$$

where  $\mathbf{J}_m$  is the nominal flux per unit area in the dry state and  $\nabla_0$  denote the gradient in the Lagrangian coordinates  $\mathbf{X}$ . Their counterparts in the actual configuration are denoted by  $\mathbf{j}_m$  and  $\nabla$  and are defined according to the following rules:

$$\mathbf{J}_m = J \mathbb{F}^{-1} \mathbf{j}_m, \quad \nabla_0(\cdot) = \mathbb{F}^T \nabla(\cdot). \quad (13)$$

When considering tissues or hydrogels, inertial and gravitational effect are commonly neglected, so that the conservation of momentum for the ECM reads:

$$\nabla_0 \cdot \mathbb{S} = 0 \quad (14)$$

$$(15)$$

where  $\mathbb{S}$  is the first Piola-Kirchoff tensor, which represents the stress state of the ECM in the initial configuration. The counterpart in the current configuration is the Cauchy stress tensor  $\mathbb{T}$ , which is related to  $\mathbb{S}$  as follows:

$$\mathbb{T} = J^{-1} \mathbb{S} \mathbb{F}^T. \quad (16)$$

The presence of free moving ions generates an electric field which is denoted by  $\mathbf{E}$  and  $\mathbf{e}$  in the initial and current configuration respectively. Introducing the electrostatic potential  $\Phi$ , we have that:

$$\mathbf{E} = -\nabla_0 \Phi, \quad \mathbf{e} = -\nabla \Phi. \quad (17)$$

As in [24], we consider the matrix to be a dielectric material. Consequently, the presence of the electric field generates an electric displacement  $\mathbf{H}$ , which must obey Gauss law of electrostatics:

$$\nabla_0 \cdot \mathbf{H} = Q, \quad (18)$$

where  $Q$  is the local total charge, which accounts for both fixed and moving charges:

$$Q = e \left( \sum_i z_i C_i + z_f C_f \right), \quad (19)$$

where  $e$  is the elementary charge,  $C_f$  is the concentration of fix charges and  $z_m$  is the valence of the corresponding charged species. Note that  $C_f$  here corresponds to the concentration of GAGs, which is assumed to be a constant a fraction of  $C_s$ . As for above, we can move from nominal quantities to the corresponding value in the current configuration by applying the following rules:

$$\mathbf{H} = J \mathbf{h} \mathbb{F}^{-T}, \quad (20)$$

$$\mathbf{E} = \mathbb{F}^T \mathbf{e}, \quad (21)$$

where  $\mathbf{h}$  is the electric displacement in the current configuration.

## 4.2 Kinematics.

As in [23], we here consider that the initial state of the system  $\mathcal{B}_0$  corresponds to the dry state of the gel. At any time  $t$ , the actual configuration of the body is  $\mathcal{B}_t$ . In this section, we want to focus on the rule according to which the body deforms from  $\mathcal{B}_0$  to  $\mathcal{B}_t$ , which depends on the properties of the system studied. In our case, we consider a poro-visco-elastic material. As shown in Figure 2, there are two mechanisms that can contribute to the change in the body conformation: a volume preserving viscous deformation and long range transport of fluid that leads to swelling.

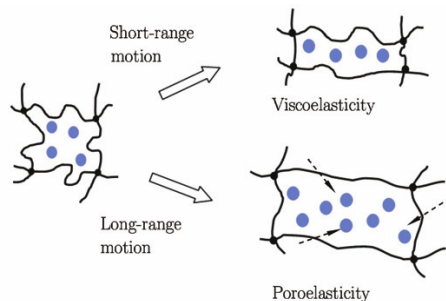


Fig. 2: Illustration of the molecular processes which account for a gel deformation: viscosity is related to change in the conformation of the network which results in short-range movement of fluid relative to the polymers; poro-elasticity is instead responsible for the long-range diffusion of solvent molecules in the gel/tissue. Reproduced from [26].

We are here interested in the coupling of this two phenomena and how information from experiment at different spatial and temporal scale can be coupled. To do so, we will here present two different approaches that have been proposed in the literature to describe the complex mechanics of hydrogels. In particular, nanoscale rheological testing with AFM usually rely on a 1D *Standard Linear Solid* model, as the one shown in Figure ??, to fit the experimental data [10,26].

As pointed out by Hu et al. [26], AFM measurements with nano-scale beads allow to capture the viscoelastic relaxation dynamics. But given the short length scale considered in the experiment, poroelastic relaxation is too fast to be captured. On the other hand, when considering larger time and spatial scale, such in standard compression test, the situation is reversed and what can be measure is the poroelastic dynamics. In this regime, the system can be well approximated by a poro-hyperelastic model [24,44]. However, we are here interested in understanding how this two aspect interplay in determining the behaviour of the tissue. In the realm of soft matter, models have been proposed that either explicitly decouple the volumetric and isochoric deformation of the system [21,36], see Figure 3(B1), or not [10,11], see Figure 3(A1). We here consider both constitutive models with the aim of comparing their predictions and identify any difference that would allow us to predict experimentally which of the two better describe the system under study. To avoid any confusion, we will denote them as model A and model B respectively. As an explanatory example of the non-



equilibrium thermodynamics framework, we will here fully derive only the first model, see Figure 3(A1). The details on the derivation of the second model can instead be found in Appendix [Need to add the name].

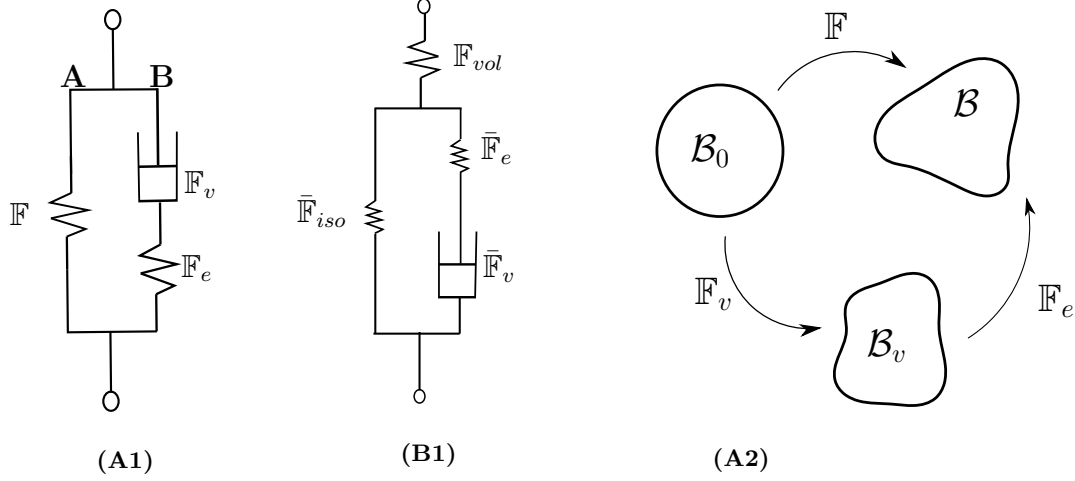


Fig. 3: (A1) Rheological model for model A; (B1) rheological model for model B; (A2) multiplicative decomposition corresponding to model A.

Following a common approach in the large-deformation theory [10,11,1,21,36,42], we base our derivation on a multiplicative decomposition of the deformation tensor  $\mathbb{F}$ , approach first proposed by Kröner in 1960 [29]:

$$\mathbb{F} = \mathbb{F}_e \mathbb{F}_v, . \quad (22)$$

As shown in Figure 3(A1),  $\mathbb{F}_e$  is the elastic contribution to the deformation, with  $J_e = \det \mathbb{F}_e > 0$ . On the other hand, the term  $\mathbb{F}_v$  accounts for the viscous part of the deformation, which arise from the local rearrangement of molecules. As illustrate in Figure 3(A2), the multiplicative decomposition is equivalent to introducing an intermediate configuration  $\mathcal{B}_v$ , called natural or virtual configuration. Despite not being a real state of the system, it can be interpreted as the state the system would be in if it was instantaneously elastically unload.

Using Equation (22), we can compute the velocity gradient tensor  $\mathbb{L}$ :

$$\mathbb{L} = \dot{\mathbb{F}} \mathbb{F}^{-1} = \mathbb{L}_e + \mathbb{F}_e \mathbb{L}_v \mathbb{F}_e^{-1}, \quad (23)$$

where  $\mathbb{L}_e = \dot{\mathbb{F}}_e \mathbb{F}_e^{-1}$  and  $\dot{\mathbb{F}}_v \mathbb{F}_v^{-1}$  are respectively the elastic and viscous velocity gradient tensor. These can be decomposed in their symmetric and skewed part:

$$\begin{aligned} \mathbb{L}_e &= \mathbb{D}_e + \mathbb{W}_e, \quad \mathbb{D}_e = \frac{\mathbb{L}_e + \mathbb{L}_e^T}{2}, \quad \mathbb{W}_e = \frac{\mathbb{L}_e - \mathbb{L}_e^T}{2}; \\ \mathbb{L}_v &= \mathbb{D}_v + \mathbb{W}_v, \quad \mathbb{D}_v = \frac{\mathbb{L}_v + \mathbb{L}_v^T}{2}, \quad \mathbb{W}_v = \frac{\mathbb{L}_v - \mathbb{L}_v^T}{2}. \end{aligned} \quad (24)$$

As mentioned before, the physical nature of the viscous deformation, molecular rearrangement, implies that  $\mathbb{F}_v$  must preserve the volume, i.e.  $J_v = \det \mathbb{F}_v = 1$ . Despite agreeing with this argument, Caccavo et al. [10,11] do not include this constraint in their mathematical formulation. Consequently, our results will differ.

Despite the additional constraint, the decomposition (22) is not unique, as  $\mathcal{B}_v$  would remained relaxed under any arbitrary rigid-body rotation [34]. As suggested by [1], in the case of isotropic material, it is reasonable to assume the viscous flow to be irrotational, i.e.  $\mathbb{W}_v = \mathbb{O}$ , so that  $\mathbb{L}_v \equiv \mathbb{D}_v$ .

### 4.3 Energy Balance Inequality.

As mentioned in Section 2, the energy imbalance inequality impose restriction on the nature of the free energy  $\psi$  of the system depending on how this exchanges energy and mass with the environment. Considering a control volume  $R$  in the reference configuration, the system exchanges mass due to diffusion of each mobile species, so that  $M(R)$  is given by:

$$M(R) = \sum_{m=s,1,\dots,N} - \int_{\partial R} \mu_m \mathbf{J}_m \cdot \mathbf{n} \quad (25)$$

where  $\mathbf{n}$  is the unit normal vector to the surface  $\partial R$  and  $\mu_m$  is the chemical potential associated with each species. Widely used in the thermodynamics of mixture, the chemical potential is a measure of the rate of change in free energy associated with adding to a unit volume one more molecule. The work done on  $R$  in the original configuration per unit time  $W(R)$  is instead made up of two contributions, the electrical  $W_{el}(R)$  and mechanical work  $W_{mec}(R)$ . Following [17],  $W_{el}(R)$  is defined as:

$$W_{el}(R) = - \int_{\partial R} \Phi \dot{\mathbf{H}} \cdot \mathbf{n} \quad (26)$$

As suggested by Gurtin [22], when accounting for the mechanical work, we consider also the effect of micro-stresses  $\boldsymbol{\epsilon}$ , which arise due to the system heterogeneity [30]. As before we consider that the dominant contribution is related to the mixing of the solvent and solid phase, so that  $W_{mec}(R)$  reads:

$$W_{mec}(R) = \int_{\partial R} (\boldsymbol{\xi} \cdot \mathbf{n}) \dot{C}_s + \int_{\partial R} \mathbb{S} \mathbf{n} \cdot \dot{\mathbf{u}} \quad (27)$$

where  $\mathbf{u} = \mathbf{x} - \mathbf{X}$  is the displacement vector, which is related to the deformation tensor,  $\mathbb{F} = \mathbb{I} - \nabla_0 \mathbf{u}$ . Substituting this result back into the energy imbalance, see Equation (2) and using the divergence theorem we obtain the following integral inequality:

$$\int_R \dot{\psi} - \mathbf{E} \cdot \dot{\mathbf{H}} + \sum_{i=1}^N \left[ e \Phi z_i \dot{C}_i + \nabla_0 (\mu_i \mathbf{J}_i) \right] + \nabla_0 (\mu_s \mathbf{J}_s - \boldsymbol{\xi} \dot{C}_s - \mathbb{S}^T \dot{\mathbf{u}}) \leq 0 \quad (28)$$

Since the above inequality must hold for any choice of the volume  $R$ , the constraint must hold locally. So that:

$$\dot{\psi} - \mathbf{E} \cdot \dot{\mathbf{H}} + \sum_{i=1}^N \left[ e\Phi z_i \dot{C}_i + \nabla_0 (\mu_i \mathbf{J}_i) \right] + \nabla_0 (\mu_s \mathbf{J}_s - \boldsymbol{\xi} \dot{C}_s - \mathbb{S}^T \dot{\mathbf{u}}) \leq 0. \quad (29)$$

Further accounting for the balance laws presented in the previous section, we obtain that:

$$\begin{aligned} \dot{\psi} - \mathbf{E} \cdot \dot{\mathbf{H}} + \sum_{i=1}^N [e\Phi z_i - \mu_i] \dot{C}_i - (\mu_s + \nabla_0 \cdot \boldsymbol{\xi}) \dot{C}_s - \mathbb{S} : \dot{\mathbb{F}} \\ - \boldsymbol{\xi} \cdot \nabla_0 \dot{C}_s + \sum_m \nabla_0 \mu_m \cdot \mathbf{J}_m \leq 0. \end{aligned} \quad (30)$$

As exhaustively discussed in [22,1], the energy imbalance inequality and the isotropic assumption on the system both impose restrictions on the constitutive equation for the free energy  $\psi$ . Adapting their results, to our specific problem, we have that:

$$\psi = \psi(\mathbb{F}, \mathbb{F}_e, C_s, C_i, \nabla C_s, \mathbf{H}). \quad (31)$$

Based on this result, we can now assign the form of the function  $\psi$ , which will problem-dependent.

#### 4.4 Construction of the Free Energy.

Following the standard approach in phase-field modeling, we assume that the total free energy is given by the superposition of each contribution. In our problem, there are six mechanisms that contributes to the energy:

- the energy of the electric field  $\psi_1$ ;
- the energy of solvent and solutes' molecules not interacting with the solid phase  $\psi_2$ ;
- the energy of mixing the solid phase with the solution,  $\psi_3$ ;
- the energy of mixing the solvent with the solutes in solution,  $\psi_4$ ;
- the interfacial energy between dissimilar phases,  $\psi_5$ ;
- the energy of the solid phase not interacting with the solution,  $\psi_6$ .

Assuming the solid phase to be an ideal and linear dielectric material, with constant permittivity  $\epsilon$ , the free energy of polarization reads [16,24]:

$$\psi_1 = \frac{1}{2\epsilon J} \mathbf{H} \mathbb{F}^T \cdot \mathbb{F} \mathbf{H}. \quad (32)$$

The specific energy density  $\psi_2$  has the standard form:

$$\psi_1 = \sum_m \mu_m^0 C_m \quad (33)$$

where  $\mu_m^0$  denote the chemical potential of non interacting solvent molecules and ions. Making use of the Flory-Huggins theory [18,27], the mixing energy is determined by the formula:

$$\psi_3 = \frac{k_B T J}{v_s} (\phi_f \ln \phi_f + \chi \phi_f \phi_n), \quad (34)$$

where  $k_B$  is the Boltzmann's constant,  $T$  is the temperature and  $\chi$  is the Flory-Huggins parameter, the adimensional parameter related to the enthalpy of mixing. It is worth mentioning also the approach of Xue et al. [43,44], where only the mixing of GAGs and solvent is assumed to contribute to the free energy. Despite GAGs having the main contribution on the swelling properties of the ECM, there is no direct experimental evidence that collagen not mixing with water. Moreover, in our model we are not explicitly differentiating between the two as separate entities, but as a unique network with fix charges, which coincide to the GAGs location.

When considering the contribution to the energy coming from the mixing of free ions with the solvent, it is commonly assumed that the solution is dilute [24,43,44], so that  $\psi_4$  reads:

$$\psi_4 = k_B T \sum_{i=1}^N C_i \left( \ln \frac{C_i}{C_s} - 1 \right). \quad (35)$$

Differently from previous work on the modelling of soft tissue, we include the effect of interface tension, which is further couple to the mechanical deformation as proposed by Hong et al. [25]. Note that as above, we assume that the contribution of ions is negligible, so that only the ideal solid-solvent interface plays a role:

$$\psi_5 = \frac{\gamma}{2} J |\nabla C_s|, \quad (36)$$

where the constant  $\gamma$  plays a role analogous to a surface tension. Finally, we need to specify the mechanical energy density  $\psi_6$ , that without any loss of generality can be decomposed as:

$$\psi_6 = \psi_{\mathbf{A}}(\mathbb{F}) + \psi_{\mathbf{B}}(\mathbb{F}_e) \quad (37)$$

where  $\mathbf{A}$  and  $\mathbf{B}$  refer to the branch of the standard linear solid model in Figure 3 (A1) which is associated with the elastic energy.

As in [44], we decide to model the collagen network as an isotropic and compressible Neo-Hookean material:

$$\psi_{\mathbf{A}}(\mathbb{F}) = \frac{G_{\mathbf{A}}}{2} (\mathbb{F} : \mathbb{F} - 3 - 2 \ln J) \quad (38)$$

$$\psi_{\mathbf{B}}(\mathbb{F}_e) = \frac{G_{\mathbf{B}}}{2} (\mathbb{F}_e : \mathbb{F}_e - 3 - 2 \ln J_e) \quad (39)$$

where  $G$  stands for the shear modulus associated with each branches, while  $J$  and  $J_e$  are as defined in the previous sections. The hyper-elastic nature of

polymers network response can be derived in the realm of statical thermodynamics, assuming Gaussian chains and an affine network model [19]. However, other thermodynamically consistent stretching energy have been proposed in the literature, which can account based on other network models [4,7,15].

#### **4.5 Entropy Production.**

## References

1. Anand, L.: A thermo-mechanically-coupled theory accounting for hydrogen diffusion and large elastic–viscoplastic deformations of metals. *International Journal of Solids and Structures* **48**(6), 962 – 971 (2011)
2. Benfenati, F., Beretta, G.P.: Ergodicity, Maximum Entropy Production, and Steepest Entropy Ascent in the Proofs of Onsager’s Reciprocal Relations. *Journal of Non Equilibrium Thermodynamics* **43**, 101–110 (Apr 2018)
3. Beretta, G.P.: The fourth law of thermodynamics: steepest entropy ascent. arXiv preprint arXiv:1908.05768 (2019)
4. Bergström, J., Boyce, M.: Constitutive modeling of the large strain time-dependent behavior of elastomers. *Journal of the Mechanics and Physics of Solids* **46**(5), 931 – 954 (1998)
5. Bertet, C., Sulak, L., Lecuit, T.: Myosin-dependent junction remodelling controls planar cell intercalation and axis elongation. *Nature* **429**, 667–71 (07 2004)
6. Biot, M.A.: General theory of three-dimensional consolidation. *Journal of Applied Physics* **12**(2), 155–164 (1941)
7. Boyce, M.C., Arruda, E.M.: Constitutive models of rubber elasticity: A review. *Rubber Chemistry and Technology* **73**(3), 504–523 (2000)
8. Buenger, D., Topuz, F., Groll, J.: Hydrogels in sensing applications. *Progress in Polymer Science* **37**(12), 1678 – 1719 (2012)
9. Butcher, D., Alliston, T., Weaver, V.: A tense situation: forcing tumour progression. *nat rev cancer* 9: 108–122. *Nature reviews. Cancer* **9**, 108–22 (03 2009)
10. Caccavo, D., Cascone, S., Lamberti, G., Barba, A.A.: Hydrogels: experimental characterization and mathematical modelling of their mechanical and diffusive behaviour. *Chem. Soc. Rev.* **47**, 2357–2373 (2018)
11. Caccavo, D., Vietri, A., Lamberti, G., Barba, A.A., Larsson, A.: Modeling the mechanics and the transport phenomena in hydrogels. In: Manca, D. (ed.) *Quantitative Systems Pharmacology, Computer Aided Chemical Engineering*, vol. 42, chap. 12, pp. 357 – 383. Elsevier (2018)
12. Chaudhuri, O.: Viscoelastic hydrogels for 3d cell culture. *Biomater. Sci.* **5**, 1480–1490 (2017)
13. Cohen Stuart, M., Huck, W., Genzer, J., Müller, M., Ober, C., Stamm, M., Sukhorukov, G., Szleifer, I., Tsukruk, V., Urban, M., Winnik, F., Zauscher, S., Luzinov, I., Minko, S.: Emerging applications of stimuli-responsive polymer materials. *Nature materials* **9**, 101–13 (2010)
14. Deligkaris, K., Tadele, T.S., Olthuis, W., Van den Berg, A.: Hydrogel-based devices for biomedical applications. *Sensors and Actuators B: Chemical* **147**, 765–774 (2010)
15. Doi, M.: *Soft Matter Physics*. OUP Oxford (2013)
16. Drozdov, A.: Swelling of ph-responsive cationic gels: Constitutive modeling and structure–property relations. *International Journal of Solids and Structures* **64–65**, 176 – 190 (2015)
17. Drozdov, A.D., deClaville Christiansen, J., Sanporean, C.G.: Inhomogeneous swelling of ph-responsive gels. *International Journal of Solids and Structures* **87**, 11 – 25 (2016)
18. Flory, P.J.: Thermodynamics of high polymer solutions. *The Journal of Chemical Physics* **10**(1), 51–61 (1942)
19. Flory, P.: *Principles of Polymer Chemistry*. Baker lectures 1948, Cornell University Press (1953)

20. Garcia-Gonzalez, D., Jerusalem, A.: Energy based mechano-electrophysiological model of cns damage at the tissue scale. *Journal of the Mechanics and Physics of Solids* **125**, 22 – 37 (2019)
21. Garcia-Gonzalez, D.: Magneto-visco-hyperelasticity for hard-magnetic soft materials: theory and numerical applications. *Smart Materials and Structures* **28**(8), 085020 (jul 2019)
22. Gurtin, M.E.: Generalized ginzburg-landau and cahn-hilliard equations based on a microforce balance. *Physica D: Nonlinear Phenomena* **92**(3), 178 – 192 (1996)
23. Hennessy, M.G., Münch, A., Wagner, B.: Surface induced phase separation of a swelling hydrogel (2018), preprint on webpage at [http://www.wias-berlin.de/preprint/2562/wias\\_preprints\\_2562.pdf](http://www.wias-berlin.de/preprint/2562/wias_preprints_2562.pdf),
24. Hong, W.: *Continuum Models of Stimuli-responsive Gels*, pp. 165–196. Springer Berlin Heidelberg, Berlin, Heidelberg (2012)
25. Hong, W., Wang, X.: A phase-field model for systems with coupled large deformation and mass transport. *Journal of the Mechanics and Physics of Solids* **61**(6), 1281 – 1294 (2013)
26. Hu, Y., Suo, Z.: Viscoelasticity and poroelasticity in elastomeric gels. *Acta Mechanica Sinica* **25**(5), 441 – 458 (2012)
27. Huggins, M.L.: Some properties of solutions of long-chain compounds. *The Journal of Physical Chemistry* **46**(1), 151–158 (1942)
28. Kondepudi, D., Prigogine, I.: *Modern Thermodynamics: From Heat Engines to Dissipative Structures*. CourseSmart, John Wiley & Sons (2014)
29. Kröner, E.: Allgemeine Kontinuumsmechanik der Versetzungen und Eigenspannungen. *Archive for Rational Mechanics and Analysis* **4**, 273–334 (1959)
30. Larché, F., Cahn, J.: The interactions of composition and stress in crystalline solids. *Acta Metallurgica* **33**(3), 331 – 357 (1985)
31. Lebon, G., Jou, D., José, C.V.: *Understanding Non-Equilibrium Thermodynamics*. Springer-Verlag Berlin Heidelberg (01 2008)
32. Levental, I., Georges, P.C., Janmey, P.A.: Soft biological materials and their impact on cell function. *Soft Matter* **3**, 299–306 (2007)
33. Li, J., Mooney, D.: Designing hydrogels for controlled drug delivery. *Nature Reviews Materials* **1**, 16071 (2016)
34. Lubarda, V.A.: Constitutive theories based on the multiplicative decomposition of deformation gradient: Thermoelasticity, elastoplasticity, and biomechanics . *Applied Mechanics Reviews* **57**(2), 95–108 (04 2004)
35. Marsland, R., England, J.: Limits of predictions in thermodynamic systems: a review. *Reports on Progress in Physics* **81**(1) (2017)
36. N’Guyen, T., Lejeunes, S., Eyheramendy, D., Boukamel, A.: A thermodynamical framework for the thermo-chemo-mechanical couplings in soft materials at finite strain. *Mechanics of Materials* **95**, 158 – 171 (2016)
37. Onsager, L.: Reciprocal relations in irreversible processes. i. *Phys. Rev.* **37**, 405–426 (Feb 1931)
38. Paszek, M.J., Zahir, N., Johnson, K.R., Lakins, J.N., Rozenberg, G.I., Gefen, A., Reinhart-King, C.A., Margulies, S.S., Dembo, M., Boettiger, D., Hammer, D.A., Weaver, V.M.: Tensional homeostasis and the malignant phenotype. *Cancer Cell* **8**(3), 241 – 254 (2005)
39. Prigogine, I.: *Introduction to thermodynamics of irreversible processes*. Interscience Publishers (1968)
40. Rauzi, M., Vérand, P., Lecuit, T., Lenne, P.F.: Nature and anisotropy of cortical forces orienting drosophila tissue morphogenesis. *Nature Cell Biology* **10**, 1401–1410 (2008)

41. Sun, D.N., Gu, W.Y., Guo, X.E., Lai, W.M., Mow, V.C.: A mixed finite element formulation of triphasic mechano-electrochemical theory for charged, hydrated biological soft tissues. *International Journal for Numerical Methods in Engineering* **45**(10), 1375–1402 (1999)
42. Xue, S.L., Li, B., Feng, X.Q., Gao, H.: Biochemomechanical poroelastic theory of avascular tumor growth. *Journal of the Mechanics and Physics of Solids* **94**, 409 – 432 (2016)
43. Xue, S.L., Li, B., Feng, X.Q., Gao, H.: A non-equilibrium thermodynamic model for tumor extracellular matrix with enzymatic degradation. *Journal of the Mechanics and Physics of Solids* **104**, 32 – 56 (2017)
44. Xue, S.L., Lin, S.Z., Li, B., Feng, X.Q.: A nonlinear poroelastic theory of solid tumors with glycosaminoglycan swelling. *Journal of Theoretical Biology* **433**, 49 – 56 (2017)
45. Yu, Y., Landis, C.M., Huang, R.: Salt-Induced Swelling and Volume Phase Transition of Polyelectrolyte Gels. *Journal of Applied Mechanics* **84**(5) (03 2017)